COMPARISON OF THE EFFECTS OF INTERNAL TEA^+ AND Cs^+ ON POTASSIUM CURRENT IN SQUID GIANT AXONS

JOHN R. CLAY
Laboratory of Biophysics, Intramural Research Program, National Institute of Neurological and Communicative Disorders and Stroke, National Institutes of Health at the Marine Biological Laboratory, Woods Hole, Massachusetts 02543

ABSTRACT Internal tetraethylammonium (TEA) and cesium ions block outward potassium current in nerve membrane in a voltage-dependent manner. Blockade with Cs^+ occurs virtually instantaneously after membrane depolarization, whereas blockade with TEA^+ occurs after a delay. The latter result suggested to Armstrong (1966, *J. Gen. Physiol.*, 50:279–293; 1969, *J. Gen. Physiol.*, 54:553–575) that potassium channels must open before TEA^+ blockade can occur, which is in contrast to Cs^+ blockade, which appears to be independent of channel gating. The results in this study concerning the effect of TEA^+ on inward (tail) current argue against the Armstrong model. Specifically, TEA^+ (partially) blocks inward current without altering the tail current time constant. This result indicates that TEA^+ can occupy its binding site within the channel whether or not the channel gates are open. This alternative hypothesis can describe both the steady-state and time-dependent components of TEA^+ blockade.

INTRODUCTION

The effects of internal cesium and tetraethylammonium ions (TEA^+) on outward potassium ion current in nerve membrane are well documented. Both ions produce voltage-dependent blockade of outward current with essentially no effect on potassium channel gating kinetics (Armstrong and Binstock, 1965; Adelman and Senft, 1966; Adelman, 1971; Armstrong and Hille, 1972; Bezanilla and Armstrong, 1972; Hille, 1975). Cesium blockade occurs virtually instantaneously after a depolarizing voltage-clamp step (Bezanilla and Armstrong, 1972), whereas TEA^+ blockade occurs in a time-dependent manner with a time constant in the 0.1- to 0.5-ms range, depending upon TEA^+ concentration (Armstrong, 1966). The latter result inspired Armstrong (1966, 1969) to propose that potassium channel gates must open before TEA^+ blockade can occur, in contrast to Cs^+ blockade, which is independent of the state of the channel gates.

The effects of internal Cs^+ and TEA^+ on inward (tail) currents have been less widely studied. Cs^+ would appear to have no effect on tail currents based on the similarity of Cs^+ blockade to that of Na^+, which has no effect on inward current (French and Wells, 1977). Blockade of inward current by internal TEA^+ clearly does occur (Koppenhöfer and Vogel, 1969; Armstrong and Hille, 1972; Fishman et al., 1984), although the implications of this result for the mechanism of TEA^+ action have not been previously described.

The results in this study confirm the above supposition concerning the lack of an effect of internal Cs^+ on tail currents and the previously published results concerning blockade of inward current by TEA^+. An assessment of the effects of TEA^+ on tail current kinetics indicates that TEA^+ blockade does occur even when channels are closed, in contrast to the Armstrong (1966, 1969) model. An alternative model is proposed in which TEA^+ blockade is independent of the channel gating mechanism (similar to Cs^+ blockade). This model is consistent with the original results of Armstrong and Binstock (1965) and Armstrong (1966), as well as the results in this report.

METHODS

Experiments were performed on voltage-clamped, internally perfused squid giant axons using methods that have been previously described (Clay and Shlesinger, 1983). The temperature in these experiments ranged between 7 and 10°C. It was maintained constant to within ±0.1°C during any single experiment. The control internal perfusate consisted of 250 mM K glutamate, 25 mM K_2HPO_4, and 370 mM sucrose. The Cs^+ perfusate consisted of 250 mM K glutamate, 25 mM K_2HPO_4, 300 mM CsF, and 55 mM sucrose. The effects of fluoride in these experiments were assessed with an internal perfusate consisting of 250 mM KF, 25 mM K_2HPO_4, and 370 mM sucrose. The TEA^+ perfusate was the same as the control with the addition of TEA-Cl powder at a final concentration of either 10 or 20 mM. Axons were superfused with artificial seawater containing either 10 or 300 mM K^+. The 10 mM KSW solution contained 430 mM NaCl and 10 mM KCl; 300 mM KSW contained 140 mM NaCl and 300 mM KCl. Both solutions also contained 50 mM $MgCl_2$, 10 mM $CaCl_2$, 10 mM Tris-HCl, and 0.5 μM tetrodotoxin (TTX). Liquid junction potentials were ≤3 mV. The results in Figs. 2 and 3 have been corrected accordingly. The potentials elsewhere represent nominal values.

The voltage-clamp protocol for axons in 10 KSW consisted of a 30 ms duration step to −30 mV followed by a 5-ms duration step to −70, −50, ... or +90 mV (Fig. 1). The potential was held at −90 mV for 5 s between each pulse sequence. The protocol for the axons in 300 mM KSW was similar, except that a 15-ms prepulse to $V = 0$ mV was used.

The current 70 μs after the second step in both protocols was used to represent the current-voltage relation of the channels activated during the prepulse, except for experiments with TEA^+ and 300 mM KSW. The current-voltage relations in these conditions were obtained by methods described below (see Results).

The results in Figs. 1 *A* and *B*, and 3 *B* are uncorrected experimental records. The results in Fig. 3 *A* and the current-voltage relations in Figs. 2 and 3 were corrected for linear leakage and capacitance currents.

RESULTS

Effects of TEA^+ and Cs^+ with 10 mM KSW

The effects of 300 mM internal Cs^+ and 20 mM TEA^+ on potassium channel current with 10 mM KSW are shown in Fig. 1. The prepulse to $V = -30$ mV activated only a small fraction of the conductance, which helped to minimize ion accumulation in the periaxonal space before the second voltage step. Outward current during the second step was blocked by Cs^+ and TEA^+ in essentially an instantaneous manner in both cases. Inward current was unaffected by Cs^+, whereas TEA^+ blocked most of the inward current through the channels activated by the prepulse. This point is further illustrated by the current-voltage relations in Fig. 2. The control results were significantly nonlinear, which is apparent by eye from the records in Fig. 1. These results were described by the Goldman-Hodgkin-Katz relation (Goldman, 1943; Hodgkin and Katz, 1949), which is given by

$$I_K^0(V) \sim V[K_o - K_i \exp(qV/kT)]/[1 - \exp(qV/kT)], \quad (1)$$

where $I_K^0(V)$ is the relative potassium current-voltage relation, V is the membrane potential, q is the electronic charge, k is the Boltzmann constant, T is absolute temperature ($q/kT \sim 25$ mV), and K_o and K_i are the external and internal potassium ion concentrations, respectively. The current-voltage relation in the presence of 300 Cs^+ was N-shaped with a region of negative slope conductance positive to $V = 0$ mV, as has been previously reported (Adelman, 1971; Bezanilla and Armstrong, 1972). A secondary increase in outward current was observed for $V > 60$ mV, which is similar to results with internal Na^+ (French and Wells, 1977). This effect suggests that Cs^+ and Na^+ are able to pass through the channel at sufficiently positive potentials (Clay and Shlesinger, 1984; French and Shoukimas, 1985). The results in Fig. 2 *A* with 300 Cs^+ for $V < 60$ mV were fitted by assuming that a cesium ion binds to a site some distance, d, within the channel ($0 \le d \le 1$). The analysis was simplified by ignoring the secondary increase in outward current for $V > 60$ mV. The steady-state current in this binding site scheme is given by (Woodhull, 1973; Blatz and Magleby, 1984).

$$I_K^B(V) = I_K^0(V)/[1 + [B^+]K_D^{-1} \exp(dqV/kT)], \quad (2)$$

where $[B^+]$ is the internal blocking ion concentration and

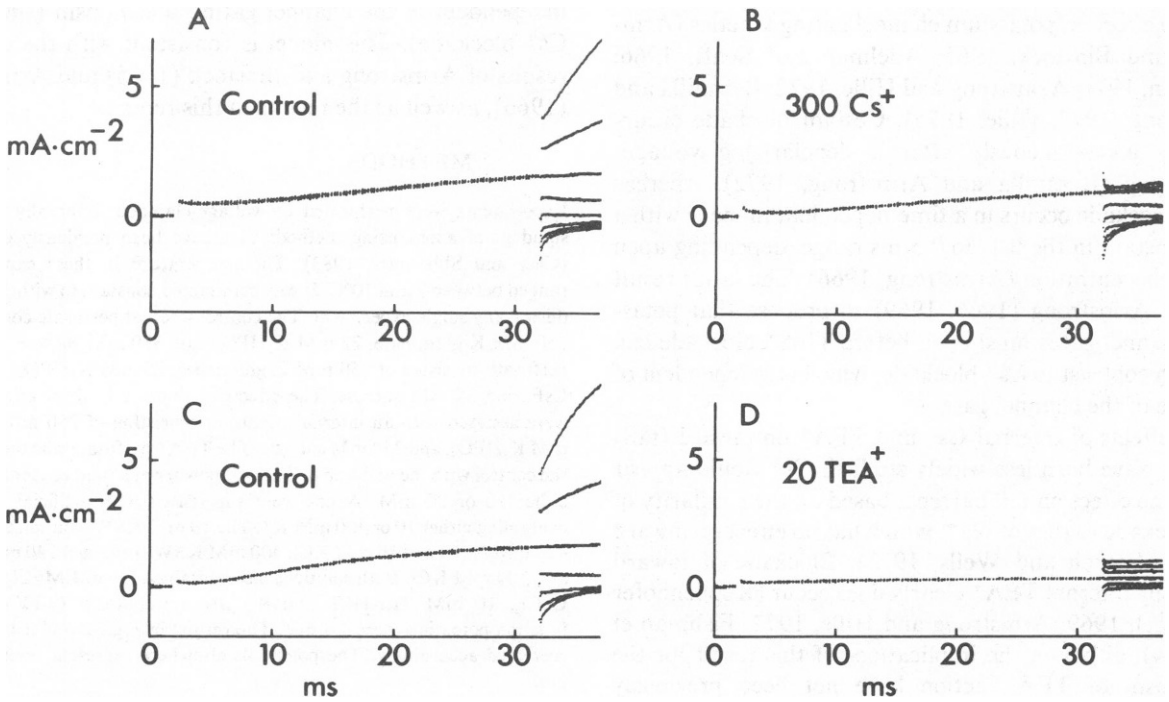

FIGURE 1 Potassium channel blockade by internal Cs^+ and TEA^+ in 10 mM KSW. (*A*) Control records for a 30-ms prepulse to −30 mV with test steps to −130, −110, −90, . . . +10 mV. Holding potential equals −90 mV. (*B*) Same as *A*, except with 300 mM CsF added to the internal perfusate. Test steps to −130, −110, . . . −10 mV. (*C*) Same protocol as in *A*. Test steps to −110, −90, . . . +10 mV. (*D*) Same as *C*, except with 20 mM TEA-Cl added to the internal perfusate. Test steps to −110, −70, −30, +10, +50, +90 mV. (*A* and *B*) Experiment C84.31. (*C* and *D*) Experiment C84.27. $T = 9$°C in both experiments. Uncorrected records.

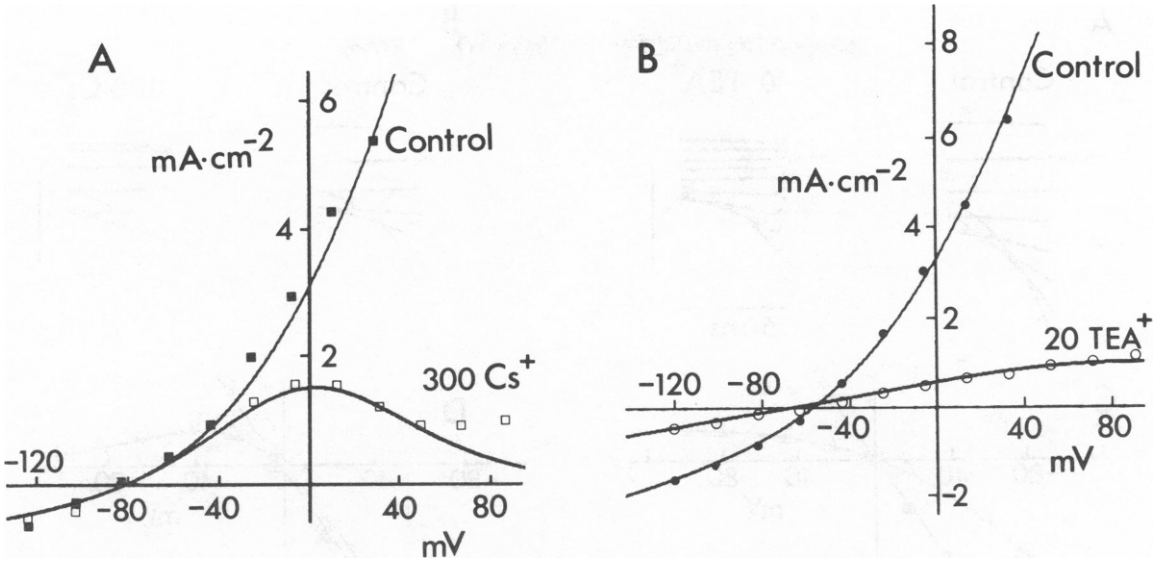

FIGURE 2 Effect of Cs^+ and TEA^+ on potassium channel current-voltage relations from the experiments shown in Fig. 1. All data points correspond to membrane current 70 μs after the test voltage step with corrections for capacitance and leakage currents. The solid lines through the control results are best fits of $I_K^0 = a\,V(K_o - K_i \exp[qV/kT])/(1 - \exp[qV/kT])$, where a is a proportionality constant and $q/kT = 25$ mV. The solid lines through the test results are best fits of $I_K^B(V) = I_K^0(V)/(1 + [B^+]K_D^{-1} \exp[dqV/kT])$, as described in the text, where $[B^+]$ is blocking ion concentration, K_D is the equilibrium dissociation constant of the blocker at zero potential, and d is the electrical distance within the channel where the blocking site is located. (*A*) Effect of Cs^+. The bulk concentration $K_o = 10$ mM was used for both theoretical curves with $K_i = 300$ mM. For the test curve $K_D = 290$ mM and $d = 0.97$. (*B*) Effect of TEA^+. $K_o = 28$ mM for the theoretical curve through the control results and $K_o = 19$ mM for the test results. $K_i = 300$ mM, $K_D = 3.95$ mM, and $d = 0.25$.

K_D is the equilibrium dissociation constant of the blocker at zero potential. The best fit values of K_D and d are given in Table I. Blockade with TEA^+ has a much broader voltage dependence compared with Cs^+, with a region of negative slope conductance positive to $V = 100$ mV (French and Shoukimas, 1981). The broader voltage dependence is apparent in Fig. 2 *B*, as well as blockade of inward current, which is the primary emphasis of this study. These results were also fitted by Eq. 2 with K_D and d given in Table I. As noted below (see Discussion), the different blocking effects of Cs^+ and TEA^+ on tail currents are attributable in the binding-site model to differences in the distances that these ions penetrate the channel.

The experiments with Cs^+ involved the addition of a significant concentration of fluoride to the internal perfusate, which has been shown to reduce potassium current (Adams and Oxford, 1983). The effect of F^- in these experiments was determined by substituting 250 KF for 250 K-glutamate in control preparations in 10 mM KSW in the absence of TTX. No effect on either the sodium current (I_{Na}) or potassium current (I_K) was observed for up to 25 min following the change of internal solution. The effects of Cs^+ in the experiment described in Figs. 1 and 2 were observed within 5 min after the addition of CsF to the internal perfusate, which is significantly less than the time required for the F^- effect to take place. Moreover, an effect of F^- would have been directly apparent in the Cs^+ experiments by a reduction in tail-current amplitude. Such an effect was not observed.

TABLE I
BLOCKING PARAMETER VALUES FOR Cs^+ AND TEA^+

K_o (mM)		Cs^+	TEA^+
10	d	0.97 ± 0.07 (±SD)	0.25
	K_D	330 ± 60 mM	4.3 mM
300	d	0.88	0.26 ± 0.02
	K_D	640 mM	3.9 ± 0.3 mM

$I_K(V) = I_K^0(V)/(1 + [B^+]K_D^{-1} \exp[qdV/kT])$, where $[B^+]$ is blocking ion concentration, and $I_K^0(V)$ is the control current-voltage relation. Each result is the average of three experiments except for TEA^+ and 10 mM K_o, and Cs^+ and 300 mM K_o: the results shown are the average of two experiments for both conditions.

Effects of TEA^+ and Cs^+ with 300 mM KSW

The effects of TEA^+ and Cs^+ on tail currents are more readily apparent in 300 mM KSW than in 10 mM KSW, because 300 mM K_o significantly increases inward current in control conditions. Moreover, the control current-voltage relation with equimolar concentrations of K^+ inside and outside the axonal membrane is a linear function of membrane potential, which simplifies the analysis of blocking ion effects. Examples of potassium current records in these control conditions and with either 10 mM TEA^+ or 300 mM Cs^+ are shown in Fig. 3. The final ~2 ms of the prepulse to $V = 0$ mM is shown in these results. The tail currents in 10 mM TEA^+ were significantly

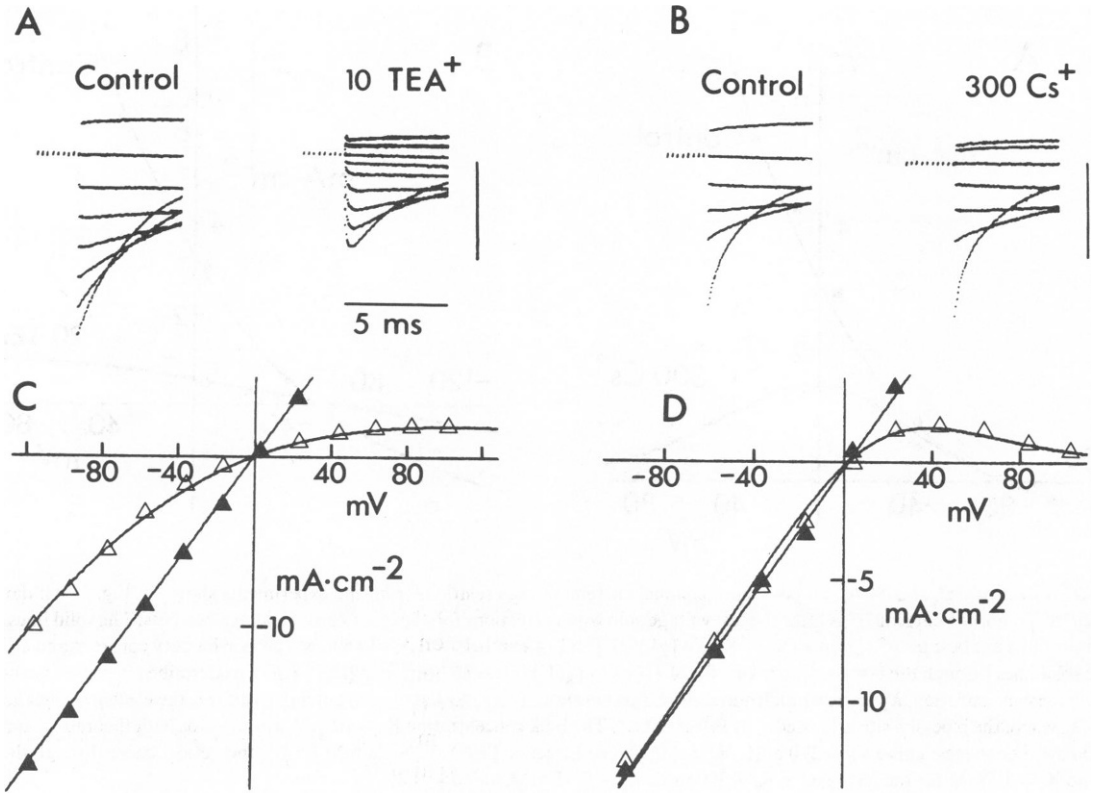

FIGURE 3 Potassium channel blockade with TEA^+ and Cs^+ in 300 mM KSW. (*A*) Control and test records for 10 mM TEA-Cl with a 20-ms prepulse to 0 mV. The last ~2 ms of the prepulse are shown here. The control records following the prepulse correspond to $V = -120$, $-100, \ldots +20$ mV. Test records correspond to V equals -120, -100, $+40$, and $+100$ mV. Vertical bar represents 10 mA · cm^{-2}. Experiment C84.26. $T = 9.5$°C. These results were corrected for capacitance and leakage currents. (*B*) Control and test records for 300 mM CsF. Same protocol as in *A*. Control records correspond to V equals -120, -80, $-60, \ldots +20$ mV. Test records correspond to $V = -120$, -80, $-60, \ldots +40$ mV. Experiment C84.32. $T = 9$°C. Uncorrected records. Vertical bar represents 10 mA · cm^{-2}. (*C*) Current-voltage relations for the TEA^+ experiment in *A*. Control data points represent membrane current 70 μs after the voltage step. The test data points were determined by extrapolating the slower time-dependent phase to zero time using the procedure described in Fig. 4. The line through the control points represents $I_K^0(V) = g_K^0 V$, where g_K^0 is a constant. The line through the test results represents $I_K^B(V) = I_K^0(V)/(1 + [B^+]K_D^{-1} \exp[dqV/kT])$, where $q/kT = 25$ mV, $[B^+]$ is TEA^+ concentration, $K_D = 3.75$ mM, and $d = 0.26$. (*D*) Current-voltage relations for the Cs^+ experiment in *B* following corrections for leakage and capacitance currents. Data points in control and after perfusion with Cs^+ represent membrane current 70 μs after the test step. The solid line through the control points represents $I_K^0(V) = g_K^0(V - E_K)$, where $E_K = 3$ mV. The solid line through the test points represents the above theoretical expression with $K_D = 570$ mM and $d = 0.98$.

reduced, whereas Cs^+ had essentially no effect on inward current, which is consistent with the corresponding results with 10 mM KSW. Moreover, time-dependent effects were apparent with TEA^+, as originally noted by Armstrong and Binstock (1965). The tail currents exhibited a slight initial increase in inward current lasting ~0.2 ms, before declining to zero. The curents for $V > 0$ mV also exhibited a slight time dependence lasting ~0.1 ms. Steady-state blockade (Fig. 3 *C*) was calculated by extrapolating the currents for $t > 0.2$ ms to the initial time of the test step as illustrated in Fig. 4 *A* for $V = -120$ mV. No time dependence was observed with Cs^+. Steady-state blockade occurred within the settling time of the voltage-clamp (≤ 50 μs). These results are shown in Fig. 3 *D*. The control current-voltage relations in Fig. 3 *C* and *D*, were fitted by $I_K^0(V) = \bar{g}_K(V - E_K)$. The TEA^+ and Cs^+ results were fitted by Eq. 2 with best fit results for K_D and d given in Table I. A notable feature of this analysis is the lack of an effect of external potassium ion concentration on TEA^+ blockade, whereas Cs^+ blockade was antagonized by K_o^+. This point is further amplified below (see Discussion).

The effects of TEA^+ on tail currents are further illustrated in Fig. 4. Both the control and the TEA^+ records for $V = -120$ mV are shown in Fig. 4 *A*. The slower, declining phase of the TEA^+ record has the same time constant as the control record, as demonstrated by multiplying the TEA^+ result by a factor (1.8) that maximizes the degree of overlap between the test and control results (Fig. 4 *B*). These results overlap almost exactly following the initial "hook" in the TEA^+ record. That is, 1/1.8, or ~55% of all channels are blocked on average at times greater than ~0.5 ms at $V = -120$ mV, even though virtually all of the channel gates are closed at this potential in steady-state. That is, TEA^+ blockade occurs whether or not the channel

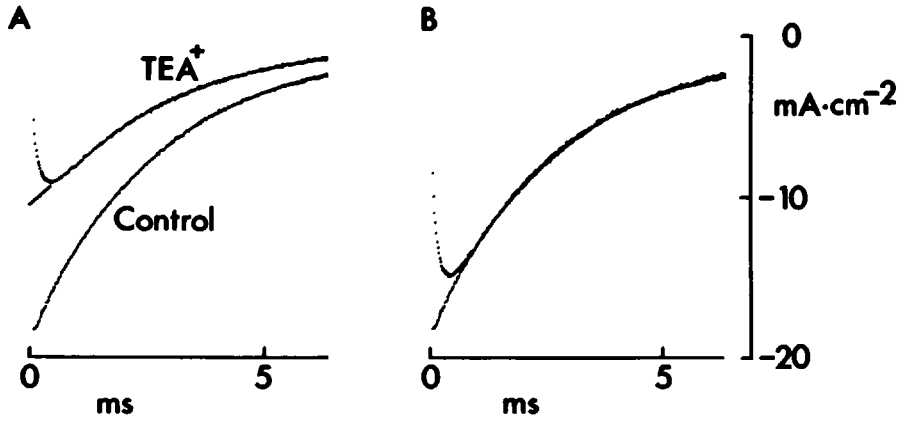

FIGURE 4 TEA^+ does not change the tail current time constant. (*A*) Control and test records for $V = -120$ mV. Same results as in Fig. 3 *A*. The solid line just below the "hook" in the TEA^+ tail record illustrates the extrapolation of the slower phase of the record to zero time. In this way steady-state block with TEA^+ at -120 mV can be estimated. (*B*) Same results as in *A* following a scaling of the TEA^+ record by a factor of 1.8.

gates are closed or open (see Discussion). Consequently, the time-dependent effects of TEA^+ can be attributed directly to the interaction between TEA^+ and its binding site within the channel, rather than an interaction between TEA^+ and the channel gating mechanism.

Time Dependence of TEA^+ Blockade

The following analysis of time-dependent TEA^+ effects is based on the description given by Woodhull (1973) for the effects of protons on sodium channels. The channel can be described by the kinetic diagram $[NB] \underset{\ell}{\overset{\kappa}{\rightleftharpoons}} [B]$, where $[B]$ represents the state of the channel when a TEA ion is located at its blocking site and $[NB]$ represents the state of the channel when a TEA ion is not bound to the blocking site. In both cases the channel gates may be either open or closed. The rate constants, κ and ℓ, are given by $\kappa = [TEA^+]\,\kappa_0 \exp(dqV/2kT)$ and $\ell = \ell_0 \exp(-dqV/2kT)$, respectively. The state of the channel is described by

$$dp_B(t) = \kappa - (\kappa + \ell)p_B(t), \tag{3}$$

where $p_B(t)$ is the probability that a channel is in its TEA^+ blocked state. The steady-state probability that any given channel is not blocked by TEA^+ is given by

$$\begin{aligned} p_{NB}(t \to \infty) &= 1 - p_B(t \to \infty) \\ &= \ell_0 \exp(-qdV/2kT)/[\ell_0 \exp(-qdV/2kT) \\ &\quad + [TEA^+]\kappa_0 \exp(qdV/2kT)] \\ &= 1/(1 + [TEA^+]K_D^{-1} \exp[qdV/kT]), \end{aligned} \tag{4}$$

with $K_D = \ell_0/\kappa_0$. Eq. 4 was used to describe the steady-state results with TEA^+ and Cs^+ (with $[TEA^+]$ replaced by $[Cs^+]$) in Figs. 2 and 3. The time constant for TEA^+ effects is given by

$$\tau_{TEA^+} = (\kappa + \ell)^{-1} = \ell_0^{-1} \exp(qdV)/2kT)/(1 + [TEA^+]K_D^{-1} \exp[qdV/kT]). \tag{5}$$

The only additional free parameter in Eq. 5, once d and K_D have been determined from the steady-state results, is ℓ_0. Experimental values for τ_{TEA^+} are given in Fig. 5. The time constant ($\tau_{TEA^+} \sim 0.15$ ms) for (partial) relief of block for $V < 0$ mV was approximately independent of voltage, which is apparent by eye from the records in Fig. 3 *A*. The value of τ_{TEA^+} for $V = 80$ or 100 mV was ~0.1 ms. No results are given in Fig. 5 for -40 mV $< V <$ 80 mV, because τ_{TEA^+} cannot be accurately determined in this voltage range for the conditions of these experiments. The theoretical curve in Fig. 5 is the best fit of Eq. 5 with $\ell_0^{-1} =$ 0.465 ms and d and K_D given in Table I. The model is consistent with the relative lack of voltage dependence of τ_{TEA^+} for -120 mV $< V < -40$ mV, even though steady-state blockade undergoes a significant change in this

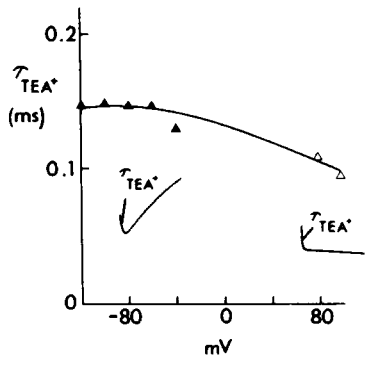

FIGURE 5 Time constant, τ_{TEA^+}, of TEA^+ effects. The data points for $V \leq -40$ mV represent the best fit single exponential time constant of the "hook" in the tail currents, as indicated by the inset. This initial time-dependent portion of the tail current is due to (partial) relief of blockade. The time constants at $V = +80$ and $+100$ mV represent best fits to the blockade at these potentials. The solid curve is the best fit to these results of $\tau_{TEA^+} = \ell_0^{-1} \exp(qdV/2kT)/(1+[TEA^+]K_D^{-1} \exp[qdV/kT])$, where K_D and d were determined from the steady-state blockade in Fig. 3 *C*. The only additional free parameter was ℓ_0^{-1}, a voltage-independent constant, which was determined to be $\ell_0^{-1} = 0.465$ ms.

potential range from $p_B(t \rightarrow \infty) = 0.43$ at $V = -120$ mV to $p_B(t \rightarrow \infty) = 0.63$ at $V = -40$ mV. The model also mimics the voltage dependence of τ_{TEA^+} between +40 and +120 mV reported by French and Shoukimas (1981) with $[TEA^+] = 1$ mM. Under these conditions τ_{TEA^+} has a bell-shaped voltage dependence with a maximal value at ~60 mV. Eq. 5 is, at least, qualitatively consistent with this observation. The model also successfully predicts the concentration dependence of TEA^+ blockade at any given potential, as illustrated in Fig. 6. The data points in Fig. 6 for $[TEA^+] = 0.6$, 1.2, and 2.4 mM represent the respective time constants of TEA^+ block at $V = +100$ mV in 440 KSW from the original measurements of Armstrong (1966). The data point at $[TEA^+] = 10$ mM was taken from this study. The solid line in Fig. 6 is the best fit to these results of Eq. 5. (The parameter ℓ_0^{-1} was changed to 0.38 ms from the value of 0.46 ms that was used in Fig. 5.) The model provides a reasonable fit to these results. In particular, it is consistent with the increased rate of blockade with increasing TEA^+ concentration, also reported by French and Shoukimas (1981).

DISCUSSION

In his original analysis of the effects of TEA^+ and related blockers of potassium channels, Armstrong (1966, 1968, 1969, 1971) hypothesized that the channel gates had to open before blockade could occur. Armstrong (1969) modeled this process by

$$[0] \underset{\beta_n}{\overset{4\alpha_n}{\rightleftharpoons}} [1] \underset{2\beta_n}{\overset{3\alpha_n}{\rightleftharpoons}} [2] \underset{3\beta_n}{\overset{2\alpha_n}{\rightleftharpoons}} [3] \underset{4\beta_n}{\overset{\alpha_n}{\rightleftharpoons}} [4] \underset{\ell}{\overset{\kappa}{\rightleftharpoons}} [4'], \qquad \text{(A)}$$

in which [0], [1], . . . [4] represent the Hodgkin and Huxley (1952) description of potassium channel gating. Their model consists of four stochastically independent, open-close gating particles, all of which must be open for ions to pass through the channel. Consequently, [4] is the only open state of Model A. Blockade by TEA^+ is represented by state [4'] and the corresponding rate constants, κ and ℓ, which describe the transitions between this state and the open state. The original motivation for Model A is best described by the effects of relatively low concentrations of TEA^+ and its derivatives on outward current (Armstrong, 1968; Armstrong and Hille, 1972; French and Shoukimas, 1981; Swenson, 1981). These results are represented schematically in Fig. 7. The control trace in Fig. 7 is an idealized description of potassium current following a step depolarization from resting membrane potential. The TEA^+ trace for a step to the same level closely follows the control, initially. It then reaches a peak value and declines in a manner suggestive of potassium channel inactivation. Both the degree and rate of inactivation (TEA^+ blockade) increase with membrane depolarization in a manner that qualitatively parallels the effect of membrane depolarization on the gating process. The idea that the gates must open for TEA^+ blockade to occur is a logical conclusion from these observations. However, these results do not necessarily require a linkage between channel activation and TEA^+ blockade. The correlation could be fortuitous, since membrane depolarization is required for both processes to occur. The results in this report favor this hypothesis. In particular, the tail current result in Fig. 4 argues against the linkage model. The forward rate constant for TEA^+ blockade, κ, in Model A is approximately equal to the backward rate constant, ℓ, at $V = -120$ mV (or other potentials in the -120 to -60 mV range) with $[TEA^+] = 10$ mM. Moreover, $\kappa \gg 4\beta_n$, where $\tau_n = (4\beta_n)^{-1}$ is the tail current time constant in control ($\alpha_n \simeq 0$ at $V = -120$ mV). Consequently, Model A predicts a significant slowing of the tail, by TEA^+, because the transition from [4] to [4'] is favored over the transition from [4] to [3]. This effect can be seen explicitly from the analytical solution to Model A with $\alpha_n = 0$, which is given by

$$P_4(t) = C_1 e^{\lambda_1 t} + C_2 e^{\lambda_2 t}, \qquad (6)$$

where C_1 and C_2 are constants that are determined from the initial conditions, $P_4(t)$ is the tail-current time course, and

$$\lambda_{1,2} = \frac{-(\kappa + \ell + 4\beta_n)}{2} \cdot [1 \pm \sqrt{1 - 16\ell\beta_n/(\kappa + \ell + 4\beta_n)^2}]. \qquad (7)$$

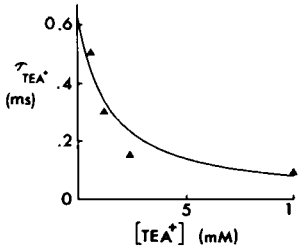

FIGURE 6 Concentration dependence of τ_{TEA^+} at V = 100 mV. The three data points for $[TEA^+] < 5$ mM were taken from Table III of Armstrong (1966). The data point at $[TEA^+] = 10$ mM was taken from this study. The solid line is the best fit to these results of Eq. 5 with $\ell_0^{-1} = 0.38$ ms.

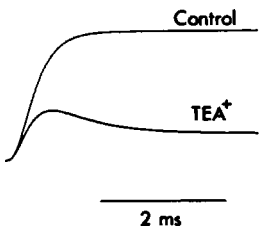

FIGURE 7 Schematic representation of the effect of TEA^+ on outward current. The control trace represents $(1 - \exp[-t/\tau])^4$ with $\tau = 0.25$ ms. The TEA^+ trace represents $(1 - \exp[-t/\tau])^4 (0.2 + 0.8 \exp[-t/\tau_2])$ with $\tau = 0.25$ ms and $\tau_2 = 0.75$ ms.

Since $\kappa \simeq \ell \gg 4\beta_n$, Eq. 7 has as its approximate solutions $\lambda_1 = -(\kappa + \ell) = -\tau_{TEA^+}^{-1}$, and $\lambda_2 = -4\beta_n\ell/(\ell + \kappa) = -\ell\tau_n^{-1}/(\ell + \kappa)$. When $\ell \simeq \kappa$, $\lambda_2 \simeq \tau_n^{-1}/2$. That is, the tail is slowed by a factor of 2. This effect is illustrated in Fig. 8 *B* with $\alpha_n = 0$, $\beta_n = 0.0482$ ms^{-1}, $\kappa = 0$ (control), or 3.08 ms^{-1}, and $\ell = 4.02$ ms^{-1}, which are parameter values corresponding to $V = -120$ mV; and $\alpha_n = 0.0975$ ms^{-1}, $\beta_n = 0.0025$ ms^{-1}, $\kappa = 0$ (control), or 5.75 ms^{-1}, and $\ell = 2.15$ ms^{-1}, which are parameter values corresponding to $V = 0$ mV. The model was assumed to be initially in steady-state conditions appropriate to $V = 0$ mV. The results in Fig. 8 *B* represent the response of the model to a step to -120 mV scaled by a factor of -17.2 mA · cm^{-2}. The control result is a single exponential, which is in close agreement with the control experimental record in Fig. 8 *A*. The TEA$^+$ result in Fig. 8 *B* displays the initial "hook" similar to that of the experimental record, but the tail is slowed significantly, as the above analysis demonstrates. The time constant is in closer agreement with experiment when κ is reduced, but then the initial blockade does not agree with experiment. In other words, Model A is logically inconsistent with the results in this report.

The most straightforward interpretation of the data in Fig. 4 *A* is that TEA$^+$ block is independent of channel gating. This model is described by

$$\begin{array}{ccccccccc} [0] & \underset{\beta_n}{\overset{4\alpha_n}{\rightleftharpoons}} & [1] & \underset{2\beta_n}{\overset{3\alpha_n}{\rightleftharpoons}} & [2] & \underset{3\beta_n}{\overset{2\alpha_n}{\rightleftharpoons}} & [3] & \underset{4\beta_n}{\overset{\alpha_n}{\rightleftharpoons}} & [4] \\ \kappa \Big\| \ell & & \kappa \Big\| \ell & & \kappa \Big\| \ell & & \kappa \Big\| \ell & & \kappa \Big\| \ell \\ [0'] & \underset{\beta_n}{\overset{4\alpha_n}{\rightleftharpoons}} & [1'] & \underset{2\beta_n}{\overset{3\alpha_n}{\rightleftharpoons}} & [2'] & \underset{3\beta_n}{\overset{2\alpha_n}{\rightleftharpoons}} & [3'] & \underset{4\beta_n}{\overset{\alpha_n}{\rightleftharpoons}} & [4'], \end{array} \qquad \text{(B)}$$

in which all of the primed states, such as [2'], refer to the state of the channel in which a TEA ion is located at its blocking site. This model is similar to the Hodgkin and Huxley (1952) model of sodium channel gating. Inactivation is independent of activation in their model just as TEA$^+$ blockade is independent of channel gating in the above model. Consequently TEA$^+$ blockade can be described by $[NB] \underset{\ell}{\overset{\kappa}{\rightleftharpoons}} [B]$ as in the analysis give in the Results. The voltage dependence of both the steady-state block and τ_{TEA^+} are a natural outcome of this model, as this study has demonstrated. The prediction of Model B for the tail-current response is given by

$$P_4(t) = A_1 e^{-t/\tau_n}(1 + A_2 e^{-t/\tau_{TEA^+}}), \qquad (8)$$

in which A_1 and A_2 are constants that are determined from the initial conditions. The predictions of Eq. 8 for the values of α_n, β_n, κ, and ℓ given above are shown in Fig. 8 *C*. These results agree closely with the experimental records in Fig. 8 *A*.

Since TEA$^+$ blockade is independent of channel gating, a similar conclusion, made on the basis of the smaller size of a Cs ion, seems reasonable for Cs$^+$ blockade. However, tail-current time constants cannot address this issue, because Cs$^+$ has virtually no blocking effect for $V \lesssim -60$ mV (Figs. 2 *A* and 3 *B*) and Models A and B give essentially identical predictions for tail current time constants when $\kappa \ll \ell$, as the above analysis demonstrates. Furthermore, both models give similar predictions for the membrane current time course following strong depolarizations. They differ significantly in the -60 to 0 mV range, which is apparent from the following simplified version of the Armstrong (1969) model, which has only a single closed state:

$$[3] \underset{\beta_n}{\overset{\alpha_n}{\rightleftharpoons}} [4] \underset{\ell}{\rightleftharpoons} [4']. \qquad \text{(C)}$$

The time constants of this model with $\ell, \kappa \gg \alpha_n, \beta_n$ are given by $(\ell + \kappa)^{-1}$ and $(\beta_n\ell/[\ell + \kappa] + \alpha_n)^{-1}$, which is equal to $(\alpha_n + \beta_n/[1 + (Cs^+)K_D^{-1} \exp(qdv/kt)])^{-1}$. That is, the

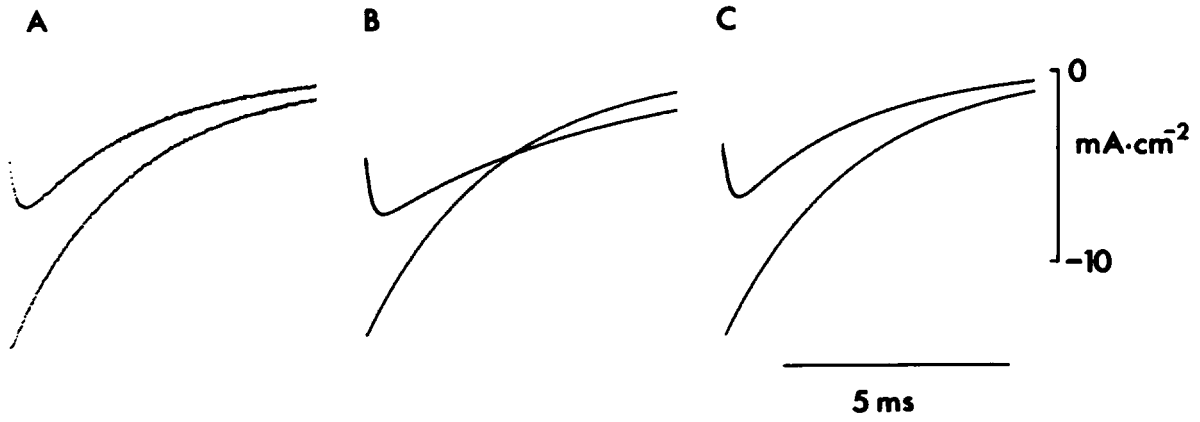

FIGURE 8 (*A*) Tail currents at -120 mV in control and following addition of 10 mM TEA$^+$ to the internal perfusate. Same records as in Fig. 4 *A*. (*B*) Prediction of Model A with β_n chosen to match the control tail current and κ and ℓ chosen to fit the initial blockade with TEA$^+$. (*C*) Prediction of Model B with β_n, κ, and ℓ the same as in Model A.

activation time constant, τ_A, in the -60 to 0 mV range is increased by Cs^+ blockade. For example, $\tau_A^{-1} \sim \alpha_n + \beta_n/2$ at $V = -30$ mV with 300 mM Cs and 10 mM K_o, and $\tau^{-1} \sim \alpha_n + \beta_n/1.5$ at $V = 0$ mV with 300 Cs and 300 K_o (Table I). Moreover, $\beta_n \sim 3\alpha_n$ at -30 mV (25% channel activation [Clay, 1984]) and $\beta_n \sim 0.25\ \alpha_n$ at 0 mV (80% channel activation [Clay, 1984]). Consequently, Model C predicts an approximate increase in τ_A of 40% at -30 mV, and 20% at 0 mV. These effects would be apparent by a reduction in tail-current amplitude. However, the results in Figs. 2 *A* and 3 *D* show virtually identical tail currents in control and following addition of Cs^+ to the internal solution. Consequently, the most straightforward interpretation of the Cs^+ results is that Cs^+ blockade is independent of channel gating.

The primary point of the Cs^+ results is that Cs^+, like Na^+, does not block inward current, in contrast to TEA^+. The results in Table I suggest the underlying reason for this difference. At a hyperpolarized potential an ion in the internal solution must have sufficient kinetic energy to overcome the barriers to outward ion movement within the channel. The blocking site for Cs^+ in the Woodhull (1973) model is 95% across the electric field of the channel, as compared to 25% for TEA^+. Consequently, the energy required for TEA^+ to reach its blocking site is considerably less than that for Cs^+. Therefore, blockade of inward current by TEA^+ at hyperpolarized potentials is more likely to occur than with Cs^+.

The results in Table I also demonstrate a lack of an effect of external potassium ion concentration on TEA^+ blockade, whereas a change in K_o from 10 to 300 mM effectively halved the blocking potency of Cs^+. These results suggest a knock-on single file diffusion character to the Cs^+ effect. In fact, a strict knock-on theoretical approach is sufficient to describe Cs^+ blockade (Clay and Shlesinger [1983, 1984]), including a slight blockade of inward current by internal Cs^+. However, knock-on theory cannot readily account for the marked effect on inward current by TEA^+. The binding site (Eyring rate theory) approach appears to be an appropriate description for these results, as this report has demonstrated.

Received for publication 28 January 1985 and in final form 5 August 1985.

REFERENCES

Adams, D. J., and G. S. Oxford. 1983. Interaction of internal anions with potassium channels of the squid axon. *J. Gen. Physiol.* 82:429–448.

Adelman, W. J., Jr. 1971. Electrical studies of internally perfused squid axons. *In* Biophysics and Physiology of Excitable Membranes. W. J. Adelman, Jr., editor. Van Nostrand Reinhold Co., New York. 274–319.

Adelman, W. J., Jr., and J. P. Senft. 1966. Voltage clamp studies on the effect of internal cesium ion on sodium and potassium currents in the squid giant axon. *J. Gen. Physiol.* 50:279–293.

Armstrong, C. M. 1966. Time course of TEA^+-induced anomalous rectification in squid giant axons. *J. Gen. Physiol.* 50:491–503.

Armstrong, C. M. 1968. Induced inactivation of the potassium permeability of squid axon membranes. *Nature (Lond.).* 219:1262–1263.

Armstrong, C. M. 1969. Inactivation of the potassium conductance and related phenomena caused by quaternary ammonium ion injection in squid axons. *J. Gen. Physiol.* 54:553–575.

Armstrong, C. M. 1971. Interaction of tetraethylammonium ion derivatives with potassium channels of giant axons. *J. Gen. Physiol.* 58:413–437.

Armstrong, C. M., and L. Binstock. 1965. Anomalous rectification in the squid giant axon injected with tetraethylammonium chloride. *J. Gen. Physiol.* 48:859–872.

Armstrong, C. M., and B. Hille. 1972. The inner quaternary ammonium ion receptor in potassium channels in the node of Ranvier. *J. Gen. Physiol.* 59:388–400.

Bezanilla, F., and C. M. Armstrong. 1972. Negative conductance caused by the entry of sodium and cesium ions into potassium channels of squid axons. *J. Gen. Physiol.* 60:588–608.

Blatz, A. L., and K. L. Magleby. 1984. Ion conductance and selectivity of single calcium-activated potassium channels in cultured rat muscle. *J. Gen. Physiol.* 84:1–23.

Clay, J. R. 1984. Potassium channel kinetics in squid axons with elevated levels of external potassium concentration. *Biophys. J.* 45:481–485.

Clay, J. R., and M. F. Shlesinger. 1983. Effects of external cesium and rubidium on outward potassium currents in squid axons. *Biophys. J.* 43:43–53.

Clay, J. R., and M. F. Shlesinger. 1984. Analysis of the effects of cesium ions on potassium channel current in biological membranes. *J. Theor. Biol.* 107:189–201.

Fishman, H. M., D. Poussart, and H. R. Leuchtag. 1984. External potassium ions alter K channel kinetics in squid axon. *Biophys. J.* 45(2, Pt. 2):141*a*. (Abstr.)

French, R. J., and J. J. Shoukimas. 1981. Blockage of squid axon potassium conductance by internal tetra-n-alkylammonium ions of various sizes. *Biophys. J.* 34:271–291.

French, R. J., and J. J. Shoukimas. 1985. An ion's view of the potassium channel. The structure of the permeation pathway as sensed by a variety of blocking ions. *J. Gen. Physiol.* 85:669–698.

French, R. J., and J. B. Wells. 1977. Sodium ions as blocking agents and charge carriers in the potassium channel of the squid giant axon. *J. Gen. Physiol.* 70:707–724.

Goldman, D. E. 1943. Potential, impedance, and rectification in membranes. *J. Gen. Physiol.* 27:37–60.

Hille, B. 1975. Ion selectivity of Na and K channels of nerve membranes. *In* Membranes: A Series of Advances. G. Eisenman, editor. Marcel Dekker, New York. 3:255–323.

Hodgkin, A. L., and A. F. Huxley. 1952. A quantitative description of membrane current and its application to conduction and excitation in nerve. *J. Physiol. (Lond.).* 117:500–544.

Hodgkin, A. L., and B. Katz. 1949. The effect of sodium ions on the electrical activity of the giant axon of the squid. *J. Physiol. (Lond.).* 108:37–77.

Koppenhöfer, E., and W. Vogel. 1969. Effects of tetrodotoxin and tetraethyl ammonium chloride on the inside of the nodal membrane of *Xenopus laevis*. *Pfluegers Arch. Eur. J. Physiol.* 313:361–380.

Swenson, R. P., Jr. 1981. Inactivation of potassium current in squid axon by a variety of quaternary ammonium ions. *J. Gen. Physiol.* 77:255–271.

Woodhull, A. M. 1973. Ionic blockage of sodium channels in nerve. *J. Gen. Physiol.* 61:687–708.